RSC Advances

PAPER

View Article Online
View Journal | View Issue

Cite this: *RSC Adv.*, 2026, **16**, 2732

Paraben adsorption on carbon-based 2D nanomaterials: molecular mechanisms and implications for environmental pollutant detection†

Deivasigamani Umadevi *

Parabens, widely used as a preservative in personal care products, have emerged as environmental micropollutants due to their persistence and endocrine disrupting potential. Insights into their interactions with nanomaterials are crucial for the rational design of effective adsorbents. In the current study, we investigated the adsorption behaviour of various paraben derivatives on carbon-based two-dimensional nanomaterials by employing a density functional theory approach. We evaluated the interactions of paraben and its alkyl derivatives with graphene and graphane, two representative carbon-based 2D nanomaterials. These substrates which differ significantly in their electronic structure and surface chemistry were used to examine the adsorption mechanisms. Our results reveal that while graphene exhibits stronger π–π interactions due to its delocalized electronic system, graphane, despite being a saturated hydrocarbon, also forms stable complexes. The strength of the binding increases as the size of the alkyl chain increases in the paraben derivatives, indicating the role of molecular size in adsorption enhancement. We also employed charge transfer calculations, topological analysis, energy decomposition analysis to further understand the nature of the interactions. This study offers molecular-level insight into paraben adsorption on nanomaterials and provides a theoretical basis for designing two-dimensional materials for selective detection and removal of organic pollutants.

Received 26th October 2025
Accepted 30th December 2025

DOI: 10.1039/d5ra08208k

rsc.li/rsc-advances

1. Introduction

Personal care products have been used for centuries for cosmetic and hygiene purposes. Synthetic chemical-based personal care products, preservatives, agricultural products and pharmaceutical products are increasing day by day as the science advances rapidly in this area. Excessive production and release of emerging contaminants by the chemical and pharmaceutical industries endanger human and other living organisms by contaminating the water resources.[1] Organic micropollutants originating from personal care and pharmaceutical products have raised increasing concern owing to their persistence in aquatic environments and potential adverse effects on ecosystems and human health.[2,3] Parabens are a class of synthetic preservatives that are most frequently used in personal care products, cosmetics and pharmaceuticals. Parabens are structurally defined as esters of *p*-hydroxybenzoic acid, consisting of an aromatic ring and variable alkyl chain lengths. They are effective at preventing microbial growth and extending the shelf life of products, however their widespread use have led to their frequent detection in various environmental sources such as surface water, groundwater *etc.*[4,5] They have the potential to interfere with hormonal systems and are classified as a group of endocrine disrupting chemicals, with the potential to cause reproductive, developmental and metabolic disorders even at trace concentrations.[6,7] Conventional wastewater treatment plants are often ineffective in completely removing parabens and related micropollutants. This ineffectiveness prompts the need for alternative remediation technologies.[8] Consequently, adsorption-based technologies using various advanced nanomaterials offer a potential approach for removing persistent organic pollutants.[9–11] Hence there is an increasing demand for effective materials for the detection of paraben contamination.

Nanotechnology offers an effective and modern approach to address the limitations of conventional treatment techniques for the removal of pollutants through efficient adsorption techniques. Nanomaterials exist in various dimensions such as zero-dimensional structures like quantum dots, one dimensional systems like nanotubes, two-dimensional structures like Mxenes and all those types were explored for adsorption studies.[12–16] Among these, two-dimensional nanomaterials have emerged as promising detection platforms owing to their thin

Department of Chemistry, Indian Institute of Technology Palakkad, Palakkad-678623, Kerala, India. E-mail: umadevi@iitpkd.ac.in; mailumaa@gmail.com

† Dedication: this article is dedicated to Professor G. Narahari Sastry on the occasion of his 60th birthday, honoring his outstanding contributions to the field of noncovalent interactions.

architecture, exceptionally high surface area, tunable surface chemistry, intrinsic porosity and unique electronic properties.[17,18] These exceptional features contribute to their superior adsorption capabilities through various mechanisms such as weak bond interactions and making them attractive for detection technologies.[19] Among the various two-dimensional nanomaterials, the carbon-based two-dimensional nanomaterials (C2DNs) such as graphene and graphane exhibit distinct advantages like high surface area, low toxicity, excellent tunability, facile functionalization and greater environmental compatibility.[20,21]

Graphene is a two-dimensional material composed of a hexagonal network of carbon atoms in sp^2 hybridization, forming a delocalized π-electron system, while graphane is the fully hydrogenated form of graphene with sp^3 hybridized carbon atoms resulting in a saturated and non-conjugated system.[22–25] The stark difference in bonding and geometry make comparing and contrasting their structural and electronic behavior scientifically interesting.[26] Graphene-based materials have been reported to be effective substrates to strongly adsorb various substrates such as gas molecules, nucleobases, amino-acids due to their unique structural features.[27–29] Graphene and its derivatives were extensively studied for the adsorptive removal of pollutants from water.[30–32] A new cellulose nanocrystal-reduced graphene oxide nanocomposite was used for electrochemical sensing of methyl paraben.[33] Despite extensive literature on graphene-based systems for pollution adsorption, comparative studies on graphane remain scarce, particularly in the context of emerging pollutants like parabens. Furthermore, the effect of alkyl chain length in parabens on their adsorption behavior towards 2D materials is not well understood. A molecular level understanding of these interactions is essential for rational material selection and design in pollutant sensing and remediation. Computational modelling serves as an important tool for elucidating the mechanism of interaction between the pollutant molecules and the nanomaterials.[34–37] Among various computational approaches, density functional theory (DFT) calculations stand out as a particularly effective method for quantitatively analyzing these interactions.[38–41] Computational modelling studies enable the identification of the key factors that contribute to the stability and specificity of adsorption processes in 2D nanomaterials.[42–48] By offering detailed molecular-level insights, these studies not only enhance our fundamental understanding of pollutant–material interactions but also provide valuable guidelines for the rational design of advanced materials tailored for desired applications.

In the current manuscript, we employed DFT to investigate the adsorption behavior of four paraben derivatives on model graphane and graphene surfaces. While previous studies have predominantly focused on the π–π interactions of pollutants with graphene like materials, our work uniquely compares the interaction profiles on both saturated and unsaturated surfaces of C2DNs. We systematically explore the binding energies, charge transfer characteristics, frontier molecular orbitals, topological descriptors and energy decomposition analysis of the systems studied which reveal key differences in interaction mechanism. Our findings provide fresh molecular-level insight into pollutant–substrate interactions and offer a theoretical foundation for the rational design of next-generation nanomaterials for environmental monitoring and water purification.

2. Computational methods and models

We modeled the C2DNs as shown in Fig. 1 and employed density functional theory (DFT) to understand their structure and properties. We used a fixed finite hydrogen-terminated

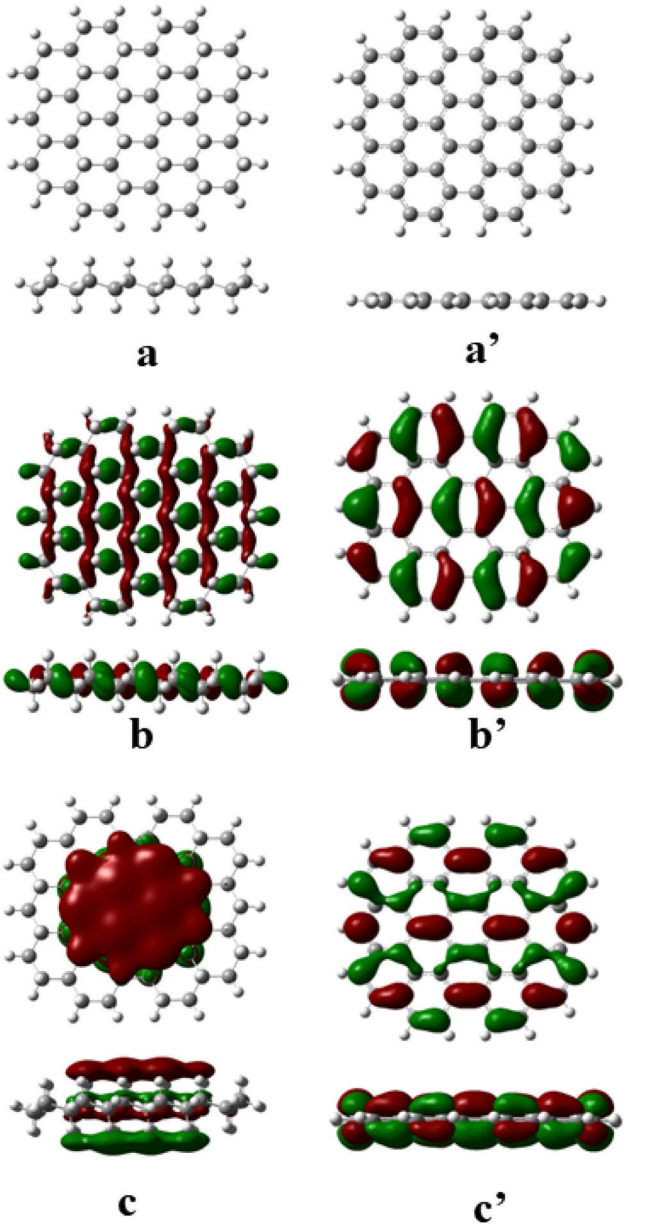

Fig. 1 Model systems to represent the carbon based 2D nanomaterials and their frontier molecular orbitals. (a) Optimized geometry of graphane (GA) (a′) Optimized geometry of graphene (GE), (b) HOMO of graphane (b′) HOMO of graphene (c) LUMO of graphane (c′) LUMO of graphene.

cluster as a representative model of the 2D material. This ensured consistent comparisons across all systems and avoided variations arising from size or edge effects. The unsaturated structure (GE) represents graphene and the saturated structure (GA) represents graphane. We added hydrogen atoms at the ends to passivate the dangling bonds in both the model systems to prevent spurious end effects. As observed in cyclohexane, graphane can also form both chair and boat shaped structures and we considered the more stable chair conformation of graphane for the current study.[23] All the geometry optimizations were carried out using the M06-2X hybrid functional of Truhlar and Zhao[49] with 6-31G (d,p) basis set as implemented in Gaussian 16 suite of programs.[50] This methodological choice was made based on the excellent performance of the M06-2X functional for noncovalent interactions, including dispersion-driven forces, π–π stacking, and CH–π interactions, which are central to the adsorption behavior of parabens on graphene and graphane. The functional has been systematically benchmarked for weak intermolecular interactions and has shown reliable accuracy for carbon nanomaterials in previous theoretical studies.[38,39] The 6-31G(d,p) basis set provides an optimal balance between computational efficiency and accurate representation of polarization effects, making it suitable for the relatively large surface models examined here. All stationary points were characterized as minima after verifying the presence of all real frequencies. We calculated the binding energy (BE) of all the complexes studied by using eqn (1),

$$\mathrm{BE} = (E_{\mathrm{C2DN}} + E_{\mathrm{PA}}) - E_{\mathrm{C2DN\text{-}PA}} \quad (1)$$

where, E_{C2DN} is the total energy of the carbon based 2D nanomaterials (GA, GE) and E_{PA} is the total energy of the parabens (PA) and $E_{\mathrm{C2DN\text{-}PA}}$ is the total energy of the carbon based 2D nanomaterials-paraben complex. We applied the counterpoise correction scheme proposed by Boys and Bernardi[51] to account for the basis set super position error (BSSE) in the binding energies calculations. We evaluated the charge transfer during the complex formation using the natural population analysis (NPA) method. In order to examine the electron density distributions, we mapped the densities at the bond critical points (BCPs) in all reported structures with the AIM2000 program.[52] We also performed energy decomposition analysis (EDA) to elucidate the nature and origin of interactions between the 2D materials and parabens, employing the Amsterdam Modeling Suite (AMS) program. EDA calculations were performed at BP86-D3(BJ)/TZ2P level using the geometries optimized at the M06-2X/6-31G (d,p) level.[53] In this approach, the total interaction energy (E_{IE}) between two interacting fragments is partitioned into four physically meaningful components, as described in eqn (2)

$$\Delta E_{\mathrm{IE}} = \Delta E_{\mathrm{Pauli}} + \Delta E_{\mathrm{Disp}} + \Delta E_{\mathrm{Elec}} + \Delta E_{\mathrm{Orb}} \quad (2)$$

where, $\Delta E_{\mathrm{Pauli}}$ is the Pauli repulsion term, ΔE_{Disp} is the dispersion component obtained as we used Grimme's D3 dispersion correction with Becke–Johnson damping, ΔE_{Elec} represents the classical electrostatic interaction between the unrelaxed fragment densities, whereas ΔE_{Orb} describes the quantum mechanical stabilization associated with orbital interaction, including polarization and charge transfer effects that occur upon relaxation of the fragment densities.[54]

3. Results and discussion

In this study, two distinct carbon-based structures were selected to model two-dimensional carbon materials (Fig. 1). The first one is a saturated hydrocarbon framework representing a graphane sheet, while the second model is an unsaturated structure mimicking a graphene sheet. DFT calculations were employed to investigate the interactions of these substrates with a series of paraben molecules, namely paraben, methyl paraben, ethyl paraben, and propyl paraben (Fig. 2). These paraben molecules were chosen due to their structural similarity, which allows for a systematic evaluation of how alkyl chain length influences adsorption behavior, binding energies, and electronic structure modifications induced by their adsorption on the surface of C2DNs. We optimized the geometries C2DNs model systems and visualized their frontier molecular orbitals (FMOs), namely the highest occupied molecular orbital (HOMO) and the lowest unoccupied molecular orbital (LUMO), as shown in Fig. 1. In graphane, the HOMO is uniformly distributed across the sheet, while the LUMO is localized predominantly at the center. In contrast, both the HOMO and LUMO orbitals of graphene are delocalized uniformly across the surface. The calculated HOMO–LUMO energy gap is significantly larger for graphane model (9.87 eV) than for graphene model (4.04 eV), indicating higher electronic stability and lower reactivity of graphane. We further computed the ionisation potentials and electron affinities of both systems. Graphane exhibits a higher ionization potential (7.59 eV) and a negative electron affinity (−2.28 eV), whereas graphene shows a lower ionization potential (5.77 eV) and a positive electron affinity (1.73 eV). These results imply that graphene is more susceptible to both electron donation and acceptance, making it more chemically reactive than graphane. The distinct electronic properties of graphane and graphene arise from differences in their orbital distribution, band gap, and charge transfer behavior. Graphene, with its delocalized frontier molecular orbitals (FMOs) and efficient charge transfer

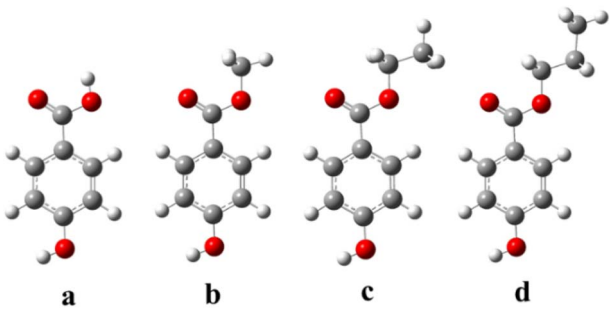

Fig. 2 Optimised structure of parabens (a) paraben, (b) methyl paraben (c) ethyl paraben and (d) propyl paraben.

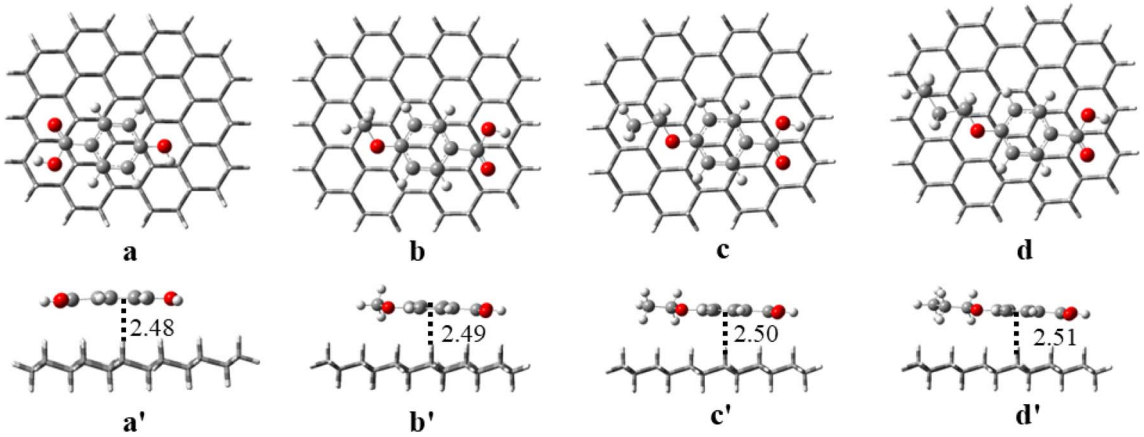

Fig. 3 Optimised structures of the complexes of graphane with various parabens with distances (Å), (a and a′) paraben, (b and b′) methyl paraben (c and c′) ethyl paraben and (d and d′) propyl paraben. The first row corresponds to the top view and the second row corresponds to the side view of the structure.

capability, readily engages in strong π–π stacking type of interactions with adsorbates such as paraben derivatives. In contrast, graphane exhibits a wider band gap and higher ionization potential indicating lower reactivity and fewer available interaction sites. These characteristics offer a theoretical basis for the observed variation in paraben adsorption on graphane and graphene, which is discussed in detail in the following sections.

3.1 Structure and geometry

In order to explore the interaction mechanisms of parabens with C2DNs, we considered various plausible orientations of the paraben molecules on both graphane and graphene model systems. To ensure a comprehensive sampling of the adsorption landscape, each paraben derivative was initially positioned in multiple geometries, including parallel, tilted, and perpendicular arrangements relative to the surface. However, during geometry optimization, all these starting orientations consistently relaxed into the same face-on stacked configuration reported in Fig. 3 and 4. No other stationary points corresponding to alternative orientations could be located, indicating that the parallel stacked geometry represents the true minimum-energy adsorption mode for all paraben derivatives on both graphane and graphene surfaces. For graphane, the optimized geometries suggest a CH–π type of interaction between the C–H moieties of the saturated graphane surface and the π-system of the aromatic ring in the paraben molecules. In the case of graphene, the optimized geometries reveal a parallel alignment between the aromatic ring of the paraben molecules and the graphene surface, indicative of classical π–π stacking. The intermolecular distances between the centroid of the aromatic ring in the paraben derivatives and the surface of the 2D nanomaterials are shown in the Fig. 3 and 4. For the graphane complexes, the centroid of the aromatic ring lies closer to the surface (~2.5 Å), which is characteristic of interactions governed by short-range dispersion contacts.[48] In contrast, the graphene complexes exhibit larger centroid-surface separations (~3.2 to 3.3 Å), consistent with typical π–π stacking geometries where the aromatic rings align parallel to the extended π-conjugated plane.[55] Thus, the relatively shorter centroid

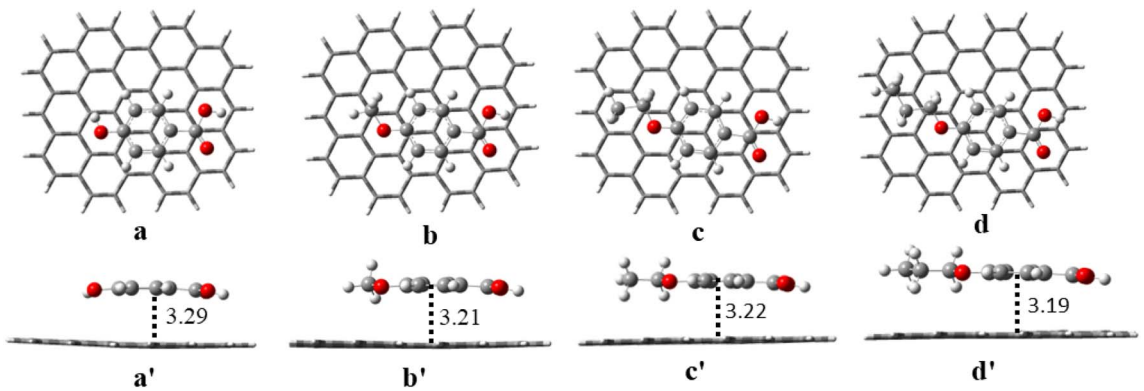

Fig. 4 Optimised structures of the complexes of graphene with various parabens with distances (Å), (a and a′) paraben, (b and b′) methyl paraben (c and c′) ethyl paraben and (d and d′) propyl paraben. The first row corresponds to the top view and the second row corresponds to the side view of the structure.

distance in graphane reflects adsorption driven by close-contact van der Waals stabilization with the hydrocarbon surface, while the larger centroid distance in graphene corresponds to π–π stacking stabilization. These structural differences reinforce that the two materials interact with parabens *via* fundamentally different noncovalent mechanisms despite adopting similar face-on orientations. The extensive delocalization of electrons in graphene allows the stacking interaction to be distributed over the entire aromatic plane rather than localized at specific atomic contacts, which contributes to the higher binding energies and stronger adsorption relative to the graphane systems. The differences in the mode of interactions and the interacting distances in the paraben's complexes with the graphane and graphene surfaces highlight the influence of surface electronic properties on adsorption behavior. In graphane, interactions mainly occur through CH–π contacts due to its saturated, sp^3-hybridised carbon atoms, which create more localized binding spots. In contrast, the sp^2-hybridised conjugated structure of graphene allows for broader, more delocalized π–π stacking interactions. These differences show how the surface chemistry of a material plays a key role in their interactions with the organic molecules. It also implies that, while both materials can bind with parabens, the type and strength of the interaction may vary depending on the electronic nature of the surface. These observations are corroborated by the binding energy calculations.

3.2 Binding energy and charge transfer

We evaluated the adsorption strength of different paraben molecules by calculating their binding energies (BEs) on both graphane and graphene surfaces. Our results reveal the across all systems, the binding energy increase with the length of the alkyl chain (propyl paraben > ethyl paraben > methyl paraben > paraben) as shown in Table 1. This indicates that bulkier parabens exhibit stronger interactions, likely due to enhanced weak interactions from greater surface contact. On graphane, the BEs range from 8.51 kcal mol^{-1} for paraben to 11.07 kcal mol^{-1} for propyl paraben. This moderate binding energy can be attributed to the CH–π type of interactions as depicted in Fig. 3.[26] Graphene shows noticeably stronger interaction with parabens ranging from 10.96 to 14.64 kcal mol^{-1}. This enhancement in binding energy can be attributed to the delocalized π-electron system in graphene, which promotes effective π–π stacking interaction with the aromatic rings of the parabens. In addition to improving adsorption energetics, this points to a higher degree of electronic interaction between the molecule and the surface. Our results also suggest that subtle variation in molecular chain such as alkyl chain length can significantly modulate adsorption behavior, offering potential pathways for designing more selective and efficient adsorbent materials.

To further probe the nature of these interactions, we performed charge transfer analysis by summing the charges of all the atoms of the parabens in the adsorbed state. A positive charge transfer values indicate the transfer of charge from parabens to C2DNs while a negative charge transfer value implies the transfer of charge from C2DNs to the parabens. On graphane, all paraben derivatives exhibit a small partial positive charge indicating the charge transfer from the paraben derivatives to graphane. This behavior aligns with the saturated and insulating character of graphane, which allows it to act as a mild electron acceptor. In contrast, adsorption on graphene results in partial negative charge on paraben derivatives implies charge transfer from graphene to the paraben derivatives. This can be attributed to the semi-metallic nature of graphene. Although the overall magnitude of charge transfer is relatively small in both cases, the clear reversal in direction highlights the fundamentally different electronic properties of graphane and graphene. Moreover, the charge transfer values remain nearly constant across the series of paraben derivatives, suggesting that variations in alkyl chain length have minimal impact on charge redistribution during adsorption.

3.3 Shapes and energies of frontier orbitals

We analyzed the highest occupied molecular orbital (HOMO) and the lowest unoccupied molecular orbital (LUMO) energy levels and their spatial distributions for the adsorbed systems to understand the electronic interactions between paraben and the C2DNs. The HOMO–LUMO energy gap (Table S3 in the SI) serves as a useful descriptor for assessing electronic stability and reactivity, while the spatial distribution of HOMO and LUMO (Fig. 5 and Fig. 6) provides insights into the nature of interactions. The HOMO–LUMO gap of the finite hydrogen-terminated clusters of graphene and graphane are larger than the bandgap of their extended system, which is a known consequence of using small molecular fragments to model 2D materials. For all graphane–paraben complexes, the HOMO is primarily localized on the graphane framework, while the LUMO is centered on the paraben molecule (Fig. 5). This indicates that the apparent reduction in the HOMO–LUMO gap of

Table 1 Binding energy (kcal mol^{-1}) and charge transfer (amu) of graphene and graphane complexes with small molecules

	Graphane		Graphene	
	Binding energy	Charge transfer	Binding energy	Charge transfer
Paraben	8.51	0.025	10.96	−0.004
Methyl paraben	9.43	0.023	12.14	−0.006
Ethyl paraben	10.11	0.018	13.17	−0.006
Propyl paraben	11.07	0.018	14.64	−0.007

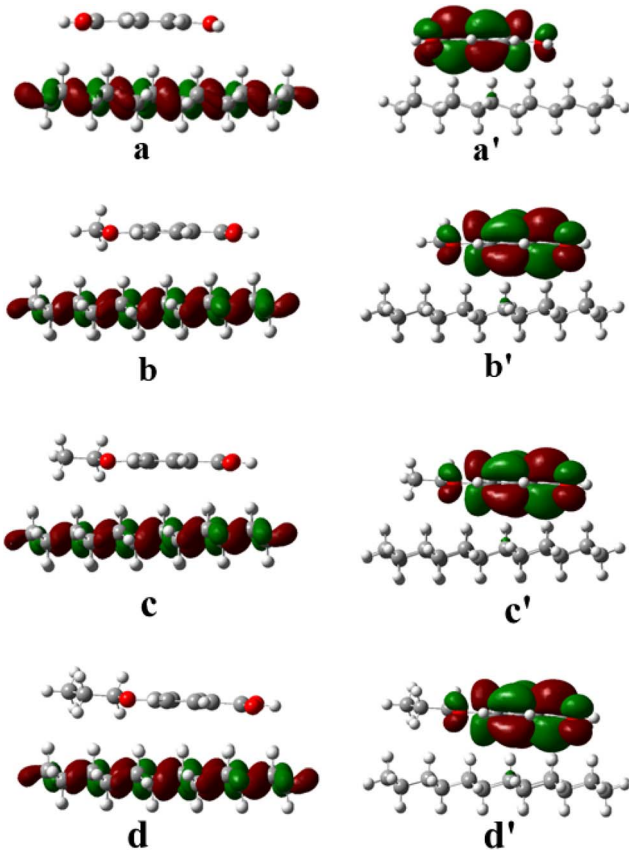

Fig. 5 Frontier molecular orbitals of the graphane complexes with (a) paraben, (b) methyl paraben, (c) ethyl paraben, and (d) propyl paraben. Panels (a–d) show the HOMO distributions, while (a′–d′) depict the corresponding LUMO distributions.

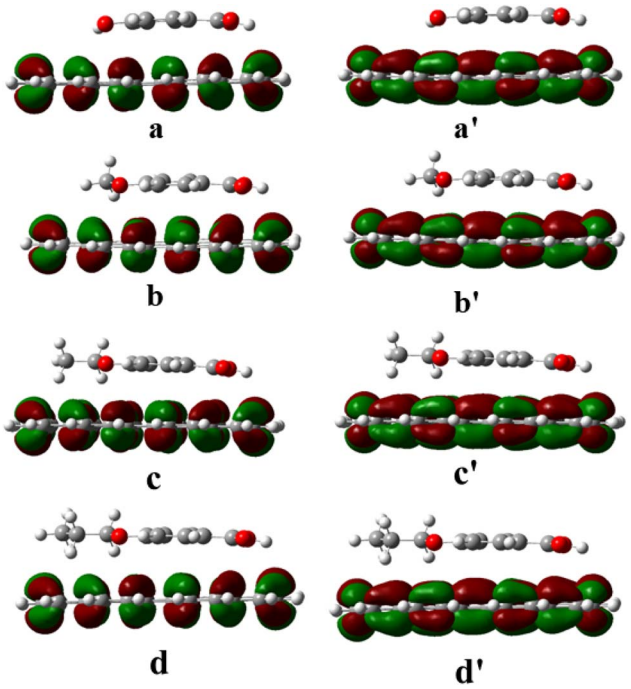

Fig. 6 Frontier molecular orbitals of the graphene complexes with (a) paraben, (b) methyl paraben, (c) ethyl paraben, and (d) propyl paraben. Panels (a–d) show the HOMO distributions, while (a′–d′) depict the corresponding LUMO distributions.

the graphane complexes arises from orbital alignment within the large gap of the finite graphane cluster, rather than from strong electronic coupling between the adsorbate and the surface. In contrast, for all graphene–paraben complexes, both the HOMO and LUMO remain delocalized over the graphene surface, with only negligible contribution from the paraben molecules (Fig. 6). This preservation of graphene-like frontier orbitals explains why the HOMO–LUMO gap of graphene complexes remains essentially unchanged and confirms that paraben adsorption induces only weak electronic perturbation, consistent with physisorption. The contrasting spatial distribution of the frontier molecular orbitals clearly highlights the electronic distinction between graphane and graphene as adsorption platforms.

3.4 Topological analysis of the electron density

We performed AIM analysis to understand the noncovalent interactions between the C2DNs and the paraben derivatives. In this framework, bond critical points, which lie along the bond path between two nuclei, were identified and analyzed as they represent the most chemically meaningful locations to characterize interactions. A key descriptor used in this analysis is the Laplacian of the electron density ($\nabla^2\rho$) which provides insight into the nature of interaction. The sign of $\nabla^2\rho$ is widely used to distinguish between shared shell (covalent) and closed shell (noncovalent or ionic) interactions. A positive Laplacian at the bond critical points (BCPs) indicates a closed shell interaction between the two centers, which may correspond to noncovalent forces or polar covalent bonding.[56,57] In all the systems studied in this work, the Laplacian values at the BCP's are positive, confirming that the interactions between the C2DNs and the paraben derivatives are predominantly of noncovalent interactions. The topology of electron density of the graphane and graphene complexes are shown in Fig. 7 and 8 respectively. As seen in Fig. 7, all the bond critical points in the graphane–paraben derivative complexes, originate from the hydrogen atoms of graphane. In contrast, in the graphene–paraben derivative complexes, the bond critical points originate from the carbon atoms of the graphene surface. This distinct difference highlights the contrasting interaction patterns of the C2DNs, as revealed by the AIM analysis. Table 2 summarizes the representative BCPs for all complexes, and the full BCP listings are provided in Tables S1 and S2 of the SI. Graphane-based systems show a larger number of BCPs with ρ values in the 0.004–0.009 a.u. range, consistent with multiple weak H⋯C contacts arising from its hydrogen-terminated surface. In contrast, graphene complexes exhibit fewer BCPs with slightly higher ρ values (0.005–0.009 a.u.), reflecting localized C⋯C(π) contacts characteristic of π–π interactions. These differences highlight the distinct interaction patterns of graphane and graphene and support the conclusion that all complexes are stabilized predominantly by weak, dispersion driven interaction.

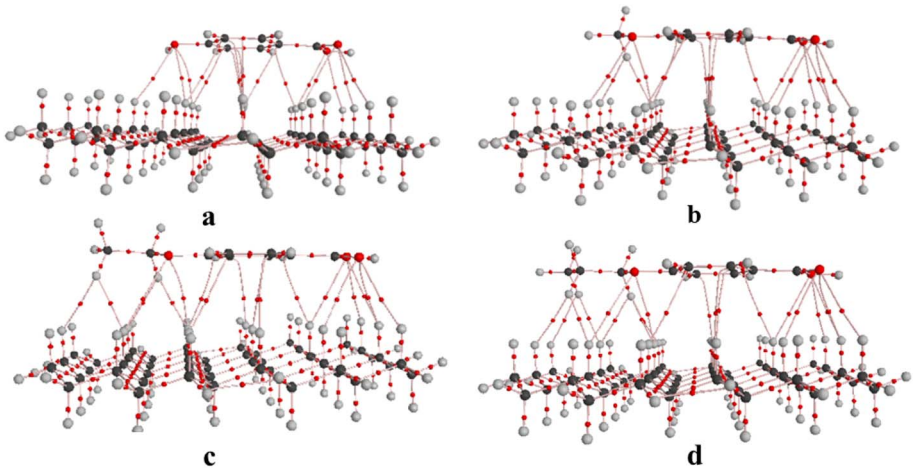

Fig. 7 Atomic positions and AIM bond critical points of graphane complexes with (a) paraben, (b) methyl paraben, (c) ethyl paraben, (d) propyl paraben.

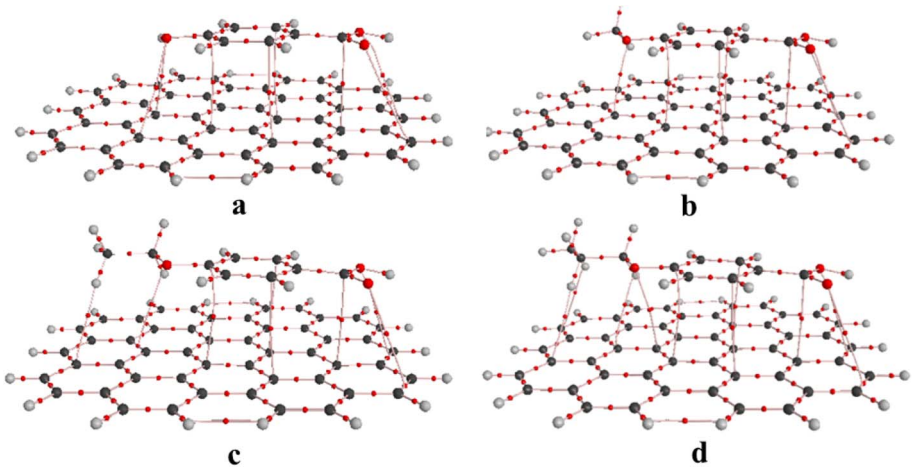

Fig. 8 Atomic positions and AIM bond critical points of graphene complexes with (a) paraben, (b) methyl paraben, (c) ethyl paraben, (d) propyl paraben.

3.5 Energy decomposition analysis

We performed energy decomposition analysis to understand the nature and origin of interactions between the C2DNs and the parabens. EDA allows us to break down the total interaction energy into physically meaningful components such as Pauli's repulsion, dispersion energy, electrostatic interaction and orbital interactions. These components provide a detailed picture of balance between stabilizing and destabilizing forces in the weak bonded complex formation. The energy components for the paraben derivatives complexes with C2DNs are given in Table 3. It is important to note that, the EDA results define the total interaction energy as negative for stabilizing interactions, hence a more negative total interaction energy indicates a stronger interaction between the C2DNs and the parabens. For graphane based systems, the total interaction energy becomes progressively more negative with increasing alkyl chain length and that confirms our observation that alkyl chains enhance the overall stabilization of the complex, primarily through weak bonded interactions. The predominant attractive contribution comes from the dispersion forces which became more pronounced with increasing molecular size. We anticipated this trend as the extended alkyl chains increase their contact area with graphane surface, amplifying London dispersion forces. The next attractive contribution comes from the electrostatic interactions but to a lesser extent. The Pauli repulsion increases slightly with molecular size, reflecting increased steric interaction between the paraben derivatives and graphane, but it is effectively countered by the increasing stabilizing components.

In the case of graphene, a similar trend of increasing total stabilization with molecular size is observed, but the magnitude of the interaction energies is significantly larger and thus consistent with our energy calculations. The dispersion energy is the dominant attractive force as observed with graphane, with larger magnitude of stabilization. The electrostatic and orbital interactions also contribute significantly, with stronger values

Table 2 Summary of representative AIM bond critical points (BCPs) for paraben adsorption on graphane (GA) and graphene (GE)[a]

Complex	No. of BCPs	ρ(BCP) range (a.u.)	Complex	No. of BCPs	ρ(BCP) range (a.u.)
GA-paraben	16	0.004–0.007	GE-paraben	8	0.006–0.008
GA-methyl paraben	16	0.004–0.008	GE-methyl paraben	7	0.006–0.009
GA-ethyl paraben	18	0.004–0.009	GE-ethyl paraben	8	0.005–0.008
GA-propyl paraben	20	0.004–0.009	GE-propyl paraben	10	0.006–0.008

[a] Full BCP listings are provided in the SI.

Table 3 Energy decomposition analysis (EDA) of paraben adsorption on graphane (GA) and graphene (GE), showing the contributions from electrostatic, Pauli repulsion, orbital, and dispersion terms to the total interaction energy (kcal mol^{-1})

	E_{Pauli}	E_{Disp}	E_{Elec}	E_{Orb}	E_{IE}
GA–paraben	24.75	−22.72	−10.37	−6.09	−14.44
GA–methyl paraben	26.74	−25.05	−11.22	−6.71	−16.24
GA–ethyl paraben	28.61	−27.06	−11.99	−7.42	−17.86
GA–propyl paraben	30.65	−29.09	−12.84	−8.08	−19.36
GE–paraben	30.60	−31.42	−14.07	−6.63	−21.51
GE–methyl paraben	32.96	−34.77	−14.71	−6.99	−23.51
GE–ethyl paraben	35.00	−37.38	−15.30	−7.63	−25.31
GE–propyl paraben	37.98	−40.30	−16.63	−8.37	−27.32

in graphene complexes indicating enhanced electronic coupling. Although Pauli repulsion is higher due to closer contact, the overall interaction remains favorable due to strong stabilizing forces. Moreover, the steady increase in stabilizing interaction energies with alkyl chain length across both C2DNs reiterates the role of molecular size and flexibility in enhancing absorption through van der Waals contact, which is an important consideration for designing surface selective adsorbents.

Although graphene exhibits stronger adsorption owing to its delocalized π-electron network, the binding energy results clearly indicate that graphane also forms remarkably stable complexes with the paraben derivatives. The underlying reason for this stability, as revealed by energy decomposition analysis (EDA), lies in the significant contributions from dispersion and electrostatic interactions, with dispersion emerging as the dominant stabilizing force, particularly enhanced by the longer alkyl chains in the parabens. These findings demonstrate that graphane, despite the absence of π-conjugation in its geometry, can effectively engage in noncovalent interactions through van der Waals and electrostatic forces. Such intrinsic stabilization highlights the potential of saturated carbon frameworks like graphane as viable and tunable materials for the adsorption of organic pollutants.

4. Conclusion

In this study, we explored the adsorption behavior of paraben derivatives on two distinct C2DNs such as graphane and graphene by employing DFT approach. Parabens, a class of widely used personal care derivatives and emerging environmental pollutants, were selected to understand how molecular structure and substrate properties influence adsorption mechanisms. Our DFT results demonstrate that both graphane and graphene can engage in noncovalent interactions with paraben derivatives, though the nature and strength of these interactions differ significantly due to their distinct surface chemistries.

Graphane, characterized by saturated hydrocarbon network and wide energy gap, interacts *via* CH–π type of interactions with modest but meaningful binding energies. In contrast, graphene with its delocalized π-electron system and quasi metallic nature, involves in stronger π–π stacking interactions. As the length of the alkyl chain increases in the paraben derivatives, the binding energies of both the C2DNs increase. Topological analysis using AIM theory confirms the noncovalent nature of all the interactions with distinct bonding patterns for graphane and graphene.

Energy decomposition analysis further substantiates these findings by identifying dispersion as the dominant attractive force in all the systems. The ability of graphane to form stable complexes with organic pollutants *via* noncovalent interactions challenges the conventional assumption that only π-conjugated systems are suitable for environmental molecule detection. These insights not only advance our understanding of the molecule–surface interactions of C2DNs but also offer valuable guidelines for developing carbon-based adsorbents or sensing platforms for the detection and removal of emerging organic pollutants like parabens. These findings also provide a useful basis for future studies aimed at improving the understanding and design of carbon-based materials for pollutant adsorption and detection. The distinct interaction patterns identified for graphene and graphane indicate that variations in surface chemistry may be exploited to tune adsorption behavior for different classes of organic contaminants. Although further computational and experimental work will be necessary to validate and extend these observations, the present results offer a helpful starting point for such investigations.

Author contributions

Umadevi Deivasigamani: conceptualization, software, resources, funding acquisition, project administration, investigation, methodology, investigation, data analysis, visualization, writing – original draft, writing – review & editing.

Conflicts of interest

There are no conflicts to declare.

Data availability

The data supporting this article have been included as part of the supplementary information (SI). Supplementary information: AIM-derived electron densities and frontier orbital energies. See DOI: https://doi.org/10.1039/d5ra08208k.

Acknowledgements

DU gratefully acknowledges the financial support from the Department of Science and Technology, Government of India, under the Women Scientist Scheme (DST WOS-A/CS-68/2021). Madhava High Performance Computing Cluster at IIT Palakkad is also sincerely acknowledged.

References

1 A. Chakraborty, S. Adhikary, S. Bhattacharya, S. Dutta, S. Chatterjee, D. Banerjee, A. Ganguly and P. Rajak, Pharmaceuticals and Personal Care Products as Emerging Environmental Contaminants: Prevalence, Toxicity, and Remedial Approaches, *ACS Chem. Health Saf.*, 2023, **30**, 362–388, DOI: 10.1021/acs.chas.3c00071.

2 R. Schwarzenbach, B. Escher, K. Fenner, T. B. Hofstetter, C. A. Johnson, U. Gunten and B. Wehrli, The Challenge of Micropollutants in Aquatic Systems, *Science*, 2006, **313**, 1072–1077, DOI: 10.1126/science.1127291.

3 S. D. Richardson and T. A. Ternes, Water Analysis: Emerging Contaminants and Current Issues, *Anal. Chem.*, 2014, **86**, 2813–2848, DOI: 10.1021/acs.analchem.9b05269.

4 S. Gonkowski, M. Tzatzarakis, N. Kadyralieva, E. Vakonaki and T. Lamprakis, Exposure assessment of dairy cows to parabens using hair samples analysis, *Sci. Rep.*, 2024, **14**, 14291, DOI: 10.1038/s41598-024-65347-z.

5 V. van der Schyff, L. Suchankov, K. Kademoglou, L. Melymuk and J. Klanova, Parabens and antimicrobial compounds in conventional and "green" personal care products, *Chemosphere*, 2022, **297**, 134019, DOI: 10.1016/j.chemosphere.2022.134019.

6 K. Nowak, W. Ratajczak-Wrona, M. Górska and E. Jablonska, Parabens and their effects on the endocrine system, *Mol. Cell. Endocrinol.*, 2018, **474**, 238–251, DOI: 10.1016/j.mce.2018.03.014.

7 R. Golden, J. Gandy and G. Vollmer, A Review of the Endocrine Activity of Parabens and Implications for Potential Risks to Human Health, *Crit. Rev. Toxicol.*, 2005, **35**(5), 435–458, DOI: 10.1080/10408440490920104.

8 F. Vale, C. A. Sousa, H. Sousa, L. Santos and M. Simoes, Parabens as emerging contaminants: Environmental persistence, current practices and treatment processes, *J. Cleaner Prod.*, 2022, **347**, 131244, DOI: 10.1016/j.jclepro.2022.131244.

9 J. Ran, M. Li, C. Zhang, F. Xue, M. Tao and W. Zhang, Synergistic Adsorption for Parabens by an Amphiphilic Functionalized Polypropylene Fiber with Tunable Surface Microenvironment, *ACS Omega*, 2020, **5**, 2920–2930, DOI: 10.1021/acsomega.9b03765.

10 Y. M. Correa-Navarro, J. D. Rivera-Giraldo and J. A. Cardona-Castaño, Modified Cellulose for Adsorption of Methylparaben and Butylparaben from an Aqueous Solution, *ACS Omega*, 2024, **9**, 30224–30233, DOI: 10.1021/acsomega.3c10304.

11 S. Su, S. Chen and C. Fan, Recent advances in two-dimensional nanomaterials-based electrochemical sensors for environmental analysis, *Green Energy Environ.*, 2018, **3**, 97e106, DOI: 10.1016/j.gee.2017.08.005.

12 A. K. I. Ahmad, Graphene quantum dots-Nascent adsorbent nanomaterials for water treatment, *Environ. Nanotechnol., Monit. Manage.*, 2024, **21**, 100943, DOI: 10.1016/j.enmm.2024.10094300.

13 M. Sajid, M. A. I. Ihsanullah, N. Baig and A. W. Mohammad, Carbon nanotubes-based adsorbents: Properties, functionalization, interaction mechanisms, and applications in water purification, *J. Water Proc. Eng.*, 2022, **47**, 102815, DOI: 10.1016/j.jwpe.2022.102815.

14 S. Massoumılari and S. Velioğlu, Can MXene be the Effective Nanomaterial Family for the Membrane and Adsorption Technologies to Reach a Sustainable Green World?, *ACS Omega*, 2023, **8**, 29859–29909, DOI: 10.1021/acsomega.3c01182.

15 Y. Zhang, L. Wang, N. Zhang and Z. Zhou, Adsorptive environmental applications of MXene nanomaterials: a review, *RSC Adv.*, 2018, **8**, 19895–19905, DOI: 10.1039/C8RA03077D.

16 B. H. Lee, J. Fatheema, D. Akinwande and W. Wang, Understanding and predicting trends in adsorption energetics on monolayer transition metal dichalcogenides, *npj 2D Mater. Appl.*, 2025, **9**, 61, DOI: 10.1038/s41699-025-00579-9.

17 D. Tyagi, H. Wang, W. Huang, L. Hu, Y. Tang, Z. Guo, Z. Ouyang and H. Zhang, Recent Advances in Two-Dimensional Materials based Sensing Technology towards Health and Environmental Applications, *Nanoscale*, 2020, **12**, 3535–3559, DOI: 10.1039/C9NR10178K.

18 N. Talreja, D. Chuahan and M. Ashfaq, Carbon-based two-dimensional (2D) materials: a next generation biocidal agent, *Mater. Adv.*, 2024, **5**, 1454–1461, DOI: 10.1039/D3MA00952A.

19 M. V. Sulleiro, A. Dominguez-Alfaro, N. Alegret, A. Silvestri and I. J. Gomez, 2D Materials towards sensing technology: From fundamentals to applications, *Sens. Biosensing Res.*, 2022, **38**, 100540, DOI: 10.1016/j.sbsr.2022.100540.

20 X. Wang and G. Shi, Introduction to the chemistry of graphene, *Phys. Chem. Chem. Phys.*, 2015, **17**, 28484–28504, DOI: 10.1039/C5CP05212B.

21 P. Kumar, R. Boukherroub and K. Shankar, Sunlight-driven water-splitting using two dimensional carbon based semiconductors, *J. Mater. Chem. A*, 2018, **6**, 12876–1293, DOI: 10.1039/C8TA02061B.

22 C. Zhou, S. Chen, J. Lou, J. Wang, Q. Yang, C. Liu, D. Huang and T. Zhu, Graphene's cousin: the present and future of graphane, *Nanoscale Res. Lett.*, 2014, **9**, 26, DOI: 10.1186/1556-276X-9-26.

23 J. O. Sofo, A. S. Chaudhari and G. D. Barber, Graphane: A two-dimensional hydrocarbon, *Phys. Rev. B*, 2007, **75**, 153401, DOI: 10.1103/PhysRevB.75.153401.
24 H. Sahin, O. Leenaerts, S. K. Singh and F. M. Peeters, Graphane, *Wiley Interdiscip. Rev.: Comput. Mol. Sci.*, 2015, **5**, 255–272, DOI: 10.1002/wcms.1216.
25 S. Demirci, T. Gorkan, E. Aktürk and S. Ciraci, Lateral Composite Structures of Graphene/Graphane/Graphone: Electronic Confinement, Heterostructures with Tunable Band Alignment, and Magnetic State, *J. Phys. Chem. C*, 2023, **127**, 17239–17248, DOI: 10.1021/acs.jpcc.3c04267.
26 D. Umadevi and G. N. Sastry, Graphane versus graphene: a computational investigation of the interaction of nucleobases, aminoacids, heterocycles, small molecules (CO_2, H_2O, NH_3, CH_4, H_2), metal ions and onium ions, *Phys. Chem. Chem. Phys.*, 2015, **17**, 30260–30269, DOI: 10.1039/C5CP05094D.
27 D. Umadevi and G. N. Sastry, Molecular and Ionic Interaction with Graphene Nanoflakes: A Computational Investigation of CO_2, H_2O, Li, Mg, Li^+, and Mg^{2+} Interaction with Polycyclic Aromatic Hydrocarbons, *J. Phys. Chem. C*, 2011, **115**, 9656–9667, DOI: 10.1021/jp201578p.
28 D. Umadevi and G. N. Sastry, Quantum Mechanical Study of Physisorption of Nucleobases on Carbon Materials: Graphene versus Carbon Nanotubes, *J. Phys. Chem. Lett.*, 2011, **2**, 1572–1576, DOI: 10.1021/jz200705w.
29 S. Yang, S. Xie, L. Tan, G. Lei, H. Xu, Z. Lan, Z. Wang and H. Gu, Selective and tunable H_2 adsorption/sensing performance of W-doped graphene under external electric fields: A DFT study, *Int. J. Hydrogen Energy*, 2022, **47**, 29579–29591, DOI: 10.1016/j.ijhydene.2022.06.259.
30 N. Baig, Ihsanullah, M. Sajid and T. A. Saleh, Graphene-based adsorbents for the removal of toxic organic pollutants: A review, *J. Environ. Manage.*, 2019, **244**, 370–382, DOI: 10.1016/j.jenvman.2019.05.047.
31 J. Wang, J. Zhang, L. Han, J. Wang, L. Zhu and H. Zeng, Graphene-based materials for adsorptive removal of pollutants from water and underlying interaction mechanism, *Adv. Colloid Interface Sci.*, 2021, **89**, 102360, DOI: 10.1016/j.cis.2021.102360.
32 D. Umadevi and G. N. Sastry, Feasibility of carbon nanomaterials as gas sensors: a computational study, *Curr. Sci.*, 2014, **106**, 1224–1234, DOI: 10.18520/CS/V106/I9/1224-1234.
33 W. E. F. W. Khalid, M. N. M. Arip, L. Jasmani and Y. H. Lee, A New Sensor for Methyl Paraben Using an Electrode Made of a Cellulose Nanocrystal–Reduced Graphene Oxide Nanocomposite, *Sensors*, 2019, **19**, 2726, DOI: 10.3390/s19122726.
34 A. Malloum, K. A. Adegoke, J. O. Ighalo, J. Conradie, *et al.*, Computational methods for adsorption study in wastewater treatment, *J. Mol. Liq.*, 2023, **390**, 123008, DOI: 10.1016/j.molliq.2023.123008.
35 K. Zhang, Z. He, K. M. Gupta and J. Jiang, Computational design of 2D functional covalent organic framework membranes for water desalination, *Environ. Sci.:Water Res. Technol.*, 2017, **3**, 735–743, DOI: 10.1039/C7EW00074J.
36 R. Pelalak, T. T. Thi, F. Golestanifar, M. Aallaei and Z. Heidari, Molecular dynamics insights into the adsorption mechanism of acidic gases over iron based metal organic frameworks, *Sci. Rep.*, 2025, **15**, 21924, DOI: 10.1038/s41598-025-07163-7.
37 Z. Gao, B. Hu, H. Wang, J. Wang and M. Cheng, Computational insights into the sorption mechanism of environmental contaminants by carbon nanoparticles through molecular dynamics simulation and density functional theory, *Phys. Chem. Chem. Phys.*, 2020, **22**, 27308, DOI: 10.1039/D0CP03459B.
38 D. Umadevi and G. N. Sastry, Metal ion binding with carbon nanotubes and graphene: Effect of chirality and curvature, *Chem. Phys. Lett.*, 2012, **549**, 39–43, DOI: 10.1016/j.cplett.2012.08.016.
39 D. Umadevi and G. N. Sastry, Impact of the Chirality and Curvature of Carbon Nanostructures on Their Interaction with Aromatics and Amino Acids, *ChemPhysChem*, 2013, **14**, 2570–2578, DOI: 10.1002/cphc.201300089.
40 S. Bhai and B. Ganguly, Probing the Interaction of Nucleobases and Fluorophore Tagged Nucleobases with Graphene Surface: Adsorption and Fluorescence Studies, *ChemistrySelect*, 2020, **5**, 3191–3200, DOI: 10.1002/slct.201904442.
41 Y. Wei, X. Liu, Z. Wang, Y. Chi, T. Yue, Y. Dai, J. Zhao and B. Xing, Adsorption and catalytic degradation of preservative parabens by graphene-family nanomaterials, *Sci. Total Environ.*, 2022, **806**, 150520, DOI: 10.1016/j.scitotenv.2021.150520.
42 S. Bhai and B. Ganguly, 2D silicene nanosheets for the detection of DNA nucleobases for genetic biomarker: a DFT study, *Struct. Chem.*, 2024, **35**, 25–37, DOI: 10.1007/s11224-023-02144-w.
43 S. Bhai and B. Ganguly, Probing the Interaction of Nucleobases and Fluorophore Tagged Nucleobases with Graphene Surface: Adsorption and Fluorescence Studies, *ChemistrySelect*, 2020, **5**, 3191–3200, DOI: 10.1002/slct.201904442.
44 J. Lazare, D. Daggag, T. Riggins, D. Boddie, R. Robinson, P. Urbaez and T. Dinadayalane, Quantum chemical study on binding of acyclic with graphene, *Next Mater.*, 2025, **9**, 101143, DOI: 10.1016/j.nxmate.2025.101143.
45 J. Lazare, D. Daggag and T. Dinadayalane, DFT study on binding of single and double methane with aromatic hydrocarbons and graphene: stabilizing CHHC interactions between two methane molecules, *Struct. Chem.*, 2021, **32**, 591–605, DOI: 10.1007/s11224-020-01657-y.
46 Y. Wei, X. Liu, Z. Wang, Y. Chi, T. Yue, Y. Dai, J. Zhao and B. Xing, Adsorption and catalytic degradation of preservative parabens by graphene-family nanomaterials, *Sci. Total Environ.*, 2022, **806**, 150520, DOI: 10.1016/j.scitotenv.2021.150520.
47 A. Yadav and S. S. Dindorkar, Vacancy defects in monolayer boron carbon nitride for enhanced adsorption of paraben compounds from aqueous stream: A quantum chemical study, *Surf. Sci.*, 2022, **723**, 122131, DOI: 10.1016/j.susc.2022.122131.

48 S. S. Dindorkar, R. V. Patel and A. Yadav, Adsorption behaviour of graphene, boron nitride and boron carbon nitride nanosheets towards pharmaceutical and personal care products, *Comput. Theor. Chem.*, 2023, **1220**, 113995, DOI: 10.1016/j.comptc.2022.113995.

49 Y. Zhao and D. G. Truhlar, The M06 suite of density functionals for main group thermochemistry, thermochemical kinetics, noncovalent interactions, excited states, and transition elements: two new functionals and systematic testing of four M06-class functionals and 12 other functionals, *Theor. Chem. Acc.*, 2008, **120**, 215, DOI: 10.1007/s00214-007-0310-x.

50 M. J. Frisch, G. W. Trucks, H. B. Schlegel, *et al. Gaussian 16, Revision C.01*, Gaussian, Inc., Wallingford CT, 2016.

51 S. F. Boys and R. Bernardi, The Calculation of Small Molecular Interactions by the Differences of Separate Total Energies. Some Procedures with Reduced Errors, *Mol. Phys.*, 1979, **19**, 553–566, DOI: 10.1080/00268977000101561.

52 F. Biegler-Knig, J. Schnbohm and D. Bayles, AIM 2000 - A Program to Analyze and Visualize Atoms in Molecules, *J. Comput. Chem.*, 2001, **22**, 545–559, DOI: 10.1002/1096-987X(20010415)22:5<545::AID-JCC1027>3.0.CO;2-Y.

53 AMS 2024.106, SCM, Theoretical Chemistry, Vrije Universiteit, Amsterdam, The Netherlands, http://www.scm.com.

54 G. Frenking and F. M. Bickelhaupt, *The Chemical Bond 1. Fundamental Aspects of Chemical Bonding, Chap. The EDA Perspective of Chemical Bonding*, Wiley-VCH, Weinheim, vol. 121, 2014.

55 D. Umadevi and G. N. Sastry, Saturated vs. unsaturated hydrocarbon interactions with carbon nanostructures, *Front. Chem.*, 2014, **2**, 75, DOI: 10.3389/fchem.2014.00075.

56 F. Cortés-Guzmán and R. F. W. Bader, Complementarity of QTAIM and MO theory in the study of bonding in donor–acceptor complexes, *Coord. Chem. Rev.*, 2005, **249**, 633–662, DOI: 10.1016/j.ccr.2004.08.022.

57 C. Foroutan-Nejad, S. Shahbazian and R. Marek, Toward a consistent interpretation of the QTAIM: Tortuous link between chemical bonds, interactions, and bond/line paths, *Chemistry*, 2014, **20**, 10140–10152, DOI: 10.1002/chem.201402177.